AIMS Mathematics, 8(3): 6447–6465.
DOI: 10.3934/math.2023326
Received: 04 October 2022
Revised: 17 November 2022
Accepted: 24 November 2022
Published: 04 January 2023

http://www.aimspress.com/journal/Math

Research article

Mathematical modeling of the COVID-19 epidemic with fear impact

Ashraf Adnan Thirthar[1], Hamadjam Abboubakar[2], Aziz Khan[3,*] and Thabet Abdeljawad[3]

[1] Department of Studies and Planning, University of Fallujah, Anbar, Iraq
[2] Department of Computer Engineering, University Institute of Technology of Ngaoundéré, The University of Ngaoundéré, P.O. Box 455, Ngaoundéré, Cameroon
[3] Department of Mathematics and Sciences, Prince Sultan University, Riyadh 11586, Saudi Arabia

* **Correspondence:** akhan@psu.edu.sa, tabdeljawad@psu.edu.sa.

Abstract: Many studies have shown that faced with an epidemic, the effect of fear on human behavior can reduce the number of new cases. In this work, we consider an SIS-B compartmental model with fear and treatment effects considering that the disease is transmitted from an infected person to a susceptible person. After model formulation and proving some basic results as positiveness and boundedness, we compute the basic reproduction number $\mathcal{R}_0$ and compute the equilibrium points of the model. We prove the local stability of the disease-free equilibrium when $\mathcal{R}_0 < 1$. We study then the condition of occurrence of the backward bifurcation phenomenon when $\mathcal{R}_0 \leq 1$. After that, we prove that, if the saturation parameter which measures the effect of the delay in treatment for the infected individuals is equal to zero, then the backward bifurcation disappears and the disease-free equilibrium is globally asymptotically stable. We then prove, using the geometric approach, that the unique endemic equilibrium is globally asymptotically stable whenever the $\mathcal{R}_0 > 1$. We finally perform several numerical simulations to validate our analytical results.

Keywords: COVID-19; mathematical model; fear effect; asymptotic stability
Mathematics Subject Classification: 37B25, 37N25, 92B05

1. Introduction

Many studies in the pathology field have shown that the effect of fear on human immunity has a direct impact on how the body produces antibodies. In human populations, the fear effect is done by media coverage of the bad effect of the disease [1,2]. The current episode of the COVID-19 pandemic is an example of how media coverage can produce a fear impact in populations. A typical example of the effect of fear on the human population's life after the beginning of the SARS outbreak is the dramatic decrease in the birth rate in Hong Kong (November 2002 to June 2003). Indeed, between 2002 to 2003,

the birth rate fell from 8,742 to 8,436 [3].

Since late 2019, the world has been preoccupied with facing a pandemic that has swept the entire world. Hundreds of thousands of people are infected every day, and tens of thousands of them die. Life stopped against her will and intense fear spread among the people. Gradually, studies on this pandemic began to expand. Many treatment protocols appeared and scientists around the world began studies to find a vaccine against this pandemic. Currently, vaccines have appeared, and a large percentage of people have taken the vaccine(see World Health Organization and [4]).

The fear factor has played an important role in the decrease in the number of deaths in the Corona epidemic thus far. Other research, on the other hand, focuses on the fact that stress causes an increase in Cortisol, which weakens immunological responses in the human body. Cortisol secretion contributes to some useful bodily processes during short periods of stress, but the problem arises when the level of Cortisol in the body is elevated for long periods of time, as it negatively affects the work of both (T-cells) and white blood cells, which has an impact on the body's immunity in general [5].

Since COVID-19 has become a pandemic, a number of mathematicians have conducted numerous studies in order to create a model and anticipate its spread. The GLM approach and Richard's model were used in the first study [6] to predict COVID-19 in China. Then, using Richard's curve, [7] estimated COVID-19 in Indonesia based on early endemic data. Other models and predictions have been widely used, such as those based on statistical techniques [8] or those based on SIS, SIR, SI1I2R, SEIR and their expansions [9]. Furthermore, several researchers modeled the spread of COVID-19 using fractional order in epidemic models. Fractional order derivative [10] and Caputo derivative [11] with the Mittag-Leffler function as a nonsingular kernel type. Then [12] looked at the fractal-fractional derivative in the Atangana-Baleanu sense to get the model's stability, and [13] used fractal-fractional operators to show the model's existence and uniqueness solution. The parameters employed in any known SIR epidemic model and its expansions, on the other hand, use crisp numbers, whereas ambiguity in parameters and population heterogeneity are extremely likely to occur. Few works were conducted to evaluate the fear effect on the transmission dynamics of COVID-19 [14]. In [15], Chandan Maji formulated and study a COVID-19 mathematical model in which the fear effect is modelized on the force of infection. He computes the basic reproduction number R_0 and proves the global stability of both equilibrium points namely the disease-free equilibrium and the endemic equilibrium. Mpeshe and Nyerere in [16] modelized the fear effect in their model by using mass action incidence coupled with the linear rate for fear effect. A statistical model was formulated and studied by Zhou et al. in [17].

In the present work, we consider the fact that new recruitment in the human population is very impacted by the COVID-19 epidemic in several regions of the world. So, we modify the traditional constant recruitment rate by including a nonlinear form of the fear effect combined with a nonlinear treatment rate. We compute the basic reproduction number $\mathcal{R}_0$ and perform the local and global stability of equilibrium points. We also prove that there is a chance that the backward bifurcation phenomenon appears in the model. Numerical simulations are conducted to validate our analytical results and to see the impact of the fear effect on the disease dynamics.

To our knowledge, few no research on the impact of fear on people with Corona has been published. As a result, we believe it is crucial to investigate this effect, which helps to lower the number of critical situations. We also used the treatment function, which is directly linked to healthy countries' capacities. In this paper, consider a COVID-19 SIS-B model that describes the dynamics of direct COVID-19 transmission, including fear effect on the susceptible individuals from infected individuals,

interactions between suspected, infected people with pathogen environment, pure death rates, vaccine effectiveness, treatment effectiveness, adherence to health protocols, treatment function and COVID-19 related deaths.

To create efficient control tactics and policies, mathematical models must be constructed in order to offer insights into the epidemic and make predictions about it [18]. Modeling approaches [19] are useful for understanding and predicting the likelihood and severity of a disease outbreak and for determining the extent to which COVID-19 disease intervention is needed. The development of new, more sophisticated versions of COVID-19 provided us with the impetus for this study, which is predicated on talking about how anxiety affects COVID-19 patients and how it contributes significantly to patient mortality.

The following is a breakdown of the paper's structure. In the next section (Section 2), we will explain the mathematical model and clarify all the hypotheses and parameters it contains. We offer some preliminaries regarding model system in Section 3, such as the positivity, boundedness of solutions, the expression of the system's basic reproduction number, the existence of steady states. The local stability of steady states analysis will also discussed in this section. Numerical simulations, used to demonstrate the analytical findings, are perform in Section 4. In the final portion, there is a brief discussion and conclusion.

2. Model formulation

In this section, we will describe and examine a COVID-19 model with fear impact combined with recovery rate, both in saturation form. We look at the entire human population sizes at time t, which comprises susceptible people $S(t)$ and infected individuals $I(t)$, designated by $N(t)$. The compartment $B(t)$ represents the pathogen population at time t.

The model implies that new recruits (including babies, travel, and so on) enter the susceptible population at a constant rate A at any given time. The model assumes that new recruits (denoted by A) people are impacted by the fear with a fear function $\dfrac{1}{1+\alpha I(t)}$, with a level of fear α. Thus the new expression of the recruitment rate is $\dfrac{A}{1+\alpha I(t)}$. The parameters β, γ, and δ describe the infection rate parameter, vaccine effectiveness parameter, and effectiveness of obedience in implementing health protocols, respectively. The death rates of S, I are μ_1, μ_2 and μ_3 is the rate of death of the virus due to sterilization with sterile substances or by the sun or the death of the virus naturally after a certain period of time. The Infection rate of free-virus in the environment is denoted by π. As a result, we consider that the recovery rate has reached its limit, and $\dfrac{aI(t)}{b+I(t)}$ is the infected compartment recovery with hospital treatment [20]. The maximum recovery per unit of time is a, and the infected size at 50% saturation is b, $h(b) = a/2$ which is a metric for how quickly saturation occurs. The parameter μ_I represents the COVID-19-related death rate. The virus concentration is increased at a rate ϵ is the Pathogen shed rate of infected individual by infected people.

In the above Figure 1 we can see a flowchart of all variables. The originality in this model is the study of the effect of fear of people infected with COVID-19 on people who are susceptible to infection using the fear function. As well as studying the effect of therapeutic protocols and their impact on disease control using the treatment function. On the other hand, the absence of compartment

B through continuous cleaning using sterilizers and detergents may contribute in one way or another to controlling and eliminating the disease.

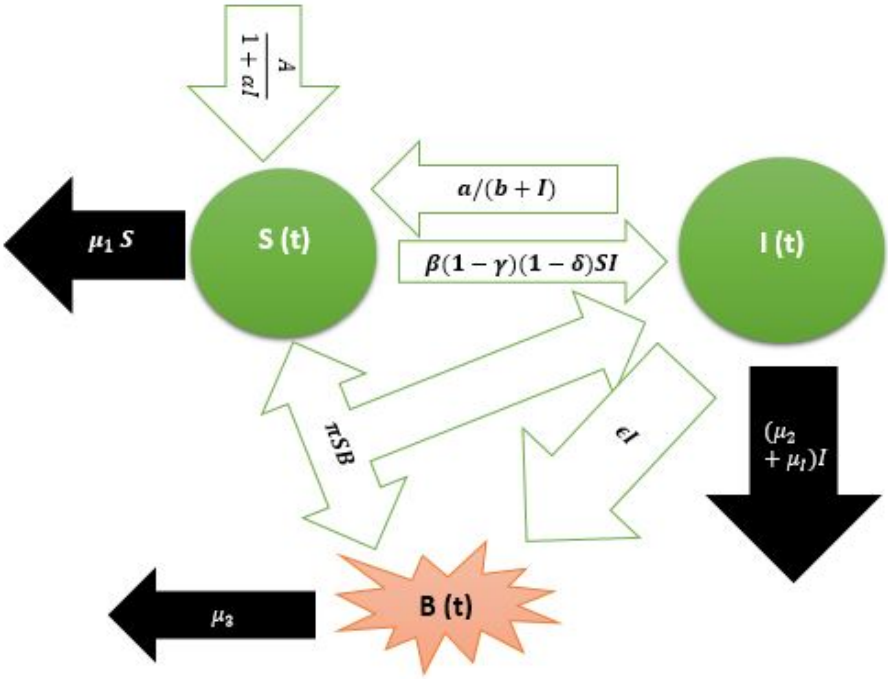

Figure 1. Flowchart of the deterministic model 2.1.

The model is mathematically stated as follows:

$$\begin{cases} \dfrac{dS}{dt}(t) = \dfrac{A}{1+\alpha I(t)} - \beta(1-\gamma)(1-\delta)S(t)I(t) - \pi S(t)B(t) - (\mu_1+\gamma+\delta)S(t) + \dfrac{aI(t)}{b+I(t)}, \\ \dfrac{dI}{dt}(t) = \beta(1-\gamma)(1-\delta)S(t)I(t) + \pi S(t)B(t) - \left(\mu_2+\mu_I+\dfrac{a}{b+I(t)}\right)I(t), \\ \dfrac{dB}{dt}(t) = \epsilon I(t) - \mu_3 B(t), \end{cases} \tag{2.1}$$

with initial conditions $S(0) > 0$, $I(0) \geq 0$, $B(0) \geq 0$.

Remark 2.1. Through the foregoing, we would like to show that $(I(t))$ is the community that contains individuals infected with COVID-19, who are actually carriers of the disease and can transmit the disease to any uninfected individual, while $(B(t))$ is the environmental elements that contain the COVID-19 virus, such as water or Hard surfaces, food, etc., which studies have shown that the virus can settle in for a period of time, and it can transmit the COVID-19 to susceptible people.

It is assumed that model parameters are non-negative and their biological meaning is described in Table 1.

Table 1. Model parameters and their description.

The Parameter	Environmental Interpretation
A	The recruitment rate
β	Infection rate parameter by I
γ	Vaccine effectiveness parameter
δ	Effectiveness of obedience in implementing health protocols
α	The level of fear
π	Infection rate parameter by B
μ_1, μ_2	The natural death rate parameters from S, I and B
μ_3	The rate of death of the virus due to sterilization with sterile substances or by the sun or the death of the virus naturally after a certain period of time.
a	The ratio of the maximum medical resource supplied per unit time to the saturation factor of the delayed in treatment
$\frac{1}{b}$	The stand for the saturation factor that measure the effect of the delay in treatment for the infected individuals
μ_I	Death rate parameter due to corona varies
ϵ	Pathogen shed rate of infected individual.

We set $x = (S, I, B)^t$ the vector of state variables and $\Sigma = \left\{x \in \mathbb{R}^3 : x \geq \mathbf{0}_{\mathbb{R}^3}\right\}$. System (2.1) can be taking the following compact form:

$$\begin{cases} \dfrac{dx}{dt} = f(x) = (f_1(x), f_2(x), f_3(x))^t, \\ x(0) = (S_0, I_0, B_0), \end{cases} \tag{2.2}$$

where $f : \mathbb{R}^3 \to \mathbb{R}^3$ is a continuously differentiable function on $\mathbb{R}^3$. According to [21, Theorem III.10.VI], for $x(0) \in \Sigma$, a unique solution of (2.1) exists, at least locally, and remains in Σ for its maximal interval of existence [21, Theorem III.10.XVI]. Hence model (2.1) is biologically well-defined.

3. Mathematical analysis

3.1. Positivity and boundedness of solutions

In this part, we study some elementary results about model (2.1), such as positivity and boundedness of model (2.1).

Theorem 3.1. *The solutions* $(S(t),\ I(t),\ B(t))$, $\forall t$, *of system* (2.1) *with initial conditions* $S(0) > 0,\ I(0)$ *and* $B(0)$ *are always positive.*

Proof. As mentioned in the study of [22], considering the non-linear system of model (2.1), we take from the first equation,

$$\frac{dS}{dt} \geq -\left[\beta(1-\gamma)(1-\delta)I(t) + \pi B(t) + (\mu_1 + \gamma + \delta)\right] S(t).$$

Integrating this equation by separation of variables, gives

$$\ln(S) \geq -\left[\beta(1-\gamma)(1-\delta)I(t) + \pi B(t) + (\mu_1 + \gamma + \delta)\right]t.$$

So on,

$$S(t) \geq S(0)\exp\left(-\left[\beta(1-\gamma)(1-\delta)I(t) + \pi B(t) + (\mu_1 + \gamma + \delta)\right]t\right).$$

Thus,

$$S(t) \geq 0.$$

Similarly, it can also been shown that $I(t) \geq 0$ and $B(t) \geq 0$. □

Theorem 3.2. *All the solutions of* (2.1) *are bounded.*

Proof. Following [23] and looking at our model (2.1), the reader will notice that it consists of two separate parts, which are human i.e, $(S(t), I(t))$ and pathogen i.e, $B(t)$ populations. Now, it's obvious from human population that:

$$\frac{d}{dt}(S(t) + I(t)) = \frac{A}{1 + \alpha I(t)} - (\mu_1 + \gamma + \delta)S(t) - (\mu_2 + \mu_I)I(t) \leq A - \kappa(S(t) + I(t)),$$

where

$$\kappa = \min\{\mu_1 + \gamma + \delta, \mu_2 + \mu_I\}.$$

Then

$$\limsup_{t\to\infty}(S + I) \leq \frac{A}{\kappa}.$$

From the pathogen class we obtain

$$\frac{dB}{dt} \leq \frac{\epsilon A}{\kappa} - \mu_3 B(t),$$

therefore,

$$B(t) \leq \frac{\epsilon A}{\kappa\mu_3}.$$

So, the solutions of model (2.1) are bounded. Through the above discussion, it will be possible to obtain the following two areas:

$$\Upsilon_H = \left\{(S, I) \in \mathbb{R}^2_+ : S + I \leq \frac{A}{\kappa}\right\} \quad \text{and} \quad \Upsilon_B = \left\{B \in \mathbb{R} : B \leq \frac{\epsilon A}{\kappa\mu_3}\right\}.$$

Let consider *int* (Υ) refers to the interior of the region Υ where $\Upsilon = \Upsilon_H \times \Upsilon_B$. Υ is a positively invariant according to model (2.1). So, the model (2.1) is well posed. □

3.2. The basic reproduction number

Model (2.1) admits a the following trivial equilibrium point $x_0 = \left(\frac{A}{(\mu_1+\gamma+\delta)}, 0, 0\right)$. According to the same appraoch described by Van den Driessche and Watmough in [24], the basic reproduction number of COVID-19 model (2.1) is defined as

$$\mathcal{R}_0 = \frac{Ab(\epsilon\pi + \beta(1-\delta)(1-\gamma)\mu_3)}{\mu_3(\mu_1+\gamma+\delta)(b(\mu_2+\mu_I)+a)}. \tag{3.1}$$

3.3. Steady states

Setting the right-hand side of system (2.1) equal to zero and solve each equation in term of I gives:

$$B^* = \frac{\epsilon}{\mu_3} I^*,\ S^* = \frac{\dfrac{I^* a}{b+I^*} + \dfrac{A}{I^*\alpha+1}}{B^*\pi + \delta_1\gamma_1 I^*\beta + k_2}, \tag{3.2}$$

where I^* is a solution of the following equation:

$$I\left(c_0 I^3 + c_1 I^2 + c_2 I + c_3\right) = 0, \tag{3.3}$$

with

$$\begin{aligned}
&c_0 = -k_1\alpha b\left(\varepsilon\pi + \delta_1\gamma_1\mu_3\beta\right),\ c_1 = -k_1 b\left(\alpha b\varepsilon\pi + \varepsilon\pi + \delta_1\gamma_1\mu_3\alpha b\beta + \delta_1\gamma_1\mu_3\beta + k_2\mu_3\alpha\right),\\
&c_2 = k_2\mu_3\left(a + k_1 b\right)\mathcal{R}_0\left[1 - \overbrace{\left(\frac{k_1 b}{A} + \frac{k_2\mu_3\left(\alpha(k_1 b + a) + k_1\right)}{A(\varepsilon\pi + \beta\delta_1\gamma_1\mu_3)}\right)}^{\mathcal{R}_c}\right],\\
&c_3 = \left(\mathcal{R}_0 - 1\right) k_2\mu_3 b\left(k_1\, b + a\right),
\end{aligned} \tag{3.4}$$

and $k_1 = \mu_2 + \mu_I$, $k_2 = \mu_1 + \gamma + \delta$, $\gamma_1 = 1 - \gamma$, $\delta_1 = 1 - \delta$.

We note that coefficients c_0 and c_1 are always negative. Coefficient c_3 is negative (resp. positive) if and only if $\mathcal{R}_0 < 1$ (resp. $\mathcal{R}_0 > 1$). The coefficient c_2 is negative (resp. positive) if and only if $\mathcal{R}_c > 1$ (resp. $\mathcal{R}_c < 1$).

Equation (3.3) has a trivial solution $I = 0$. Replacing $I = 0$ in (3.2), we obtain the disease-free equilibrium point x_0. Now we consider that $I > 0$. According to the Descartes' rule of sign, we are able to claim the following result:

Theorem 3.3. *COVID-19 model* (2.1) *admits:*

(i) the disease-free equilibrium x_0 as unique biological feasible steady state if and only if $\mathcal{R}_0 \leq 1$ and $\mathcal{R}_c > 1$;

(ii) a co-existence between the disease-free equilibrium x_0 and two endemic equilibrium points as the only possible three steady states if $\mathcal{R}_0 < 1$ and $\mathcal{R}_c < 1$;

(iii) a co-existence between the disease-free equilibrium x_0 and an endemic equilibrium as the only two steady states if $\mathcal{R}_0 = 1$ and $\mathcal{R}_c < 1$;

(iv) a co-existence between the disease-free equilibrium x_0 and an endemic equilibrium point as the two only possible steady states if $\mathcal{R}_0 > 1$.

3.4. Local stability analysis of the disease-free equilibrium and backward bifurcation condition

Let us denote by $x^* = (S^*, I^*, B^*)$ an arbitrary steady state of model (2.1). The Jacobian matrix of (2.1) evaluated at x^* is given by

$$\mathcal{J}(x^*) = \begin{pmatrix} -\beta\gamma_1\delta_1 I^* - \pi B^* - k_2, & -\dfrac{\alpha A}{(1+\alpha I^*)^2} - \beta\gamma_1\delta_1 S^* + \dfrac{ab}{(b+I^*)^2}, & -\pi S^* \\ \beta\gamma_1\delta_1 I^* + \pi B^*, & \beta\gamma_1\delta_1 S^* - k_1 - \dfrac{ab}{(b+I^*)^2}, & \pi S^* \\ 0, & \varepsilon, & -\mu_3 \end{pmatrix}. \tag{3.5}$$

At the disease-free equilibrium, i.e, $I^* = 0$, the characteristic equation of $\mathcal{J}(x_0)$ is given by

$$(X + k_2)\overbrace{\left(\varpi_2 X^2 + \varpi X + \varpi_0\right)}^{P(X)} = 0, \tag{3.6}$$

where

$$\begin{aligned} \varpi_2 &= b(\varepsilon\pi + \delta_1\gamma_1\mu_3\beta), \\ \varpi_1 &= ((\mu_3 + k_1)b + a)\varepsilon\pi + \left(\left(\delta_1\gamma_1\mu_3^2 + (1-\mathcal{R}_0)\delta_1 k_1\gamma_1\mu_3\right)b + (1-\mathcal{R}_0)\delta_1\gamma_1\mu_3 a\right)\beta, \\ \varpi_0 &= (1-\mathcal{R}_0)\mu_3(k_1 b + a)(\varepsilon\pi + \delta_1\gamma_1\mu_3\beta). \end{aligned} \tag{3.7}$$

Solutions of Eq (3.6) is $X = -k_2$ and those of $P(X)$. Since all coefficient of $P(X)$ is always positive whenever $\mathcal{R}_0 < 1$, it follows that solutions of $P(X)$ has roots with negative real parts. Thus we conclude that all the eigenvalues of the Jacobian matrix of model (2.1) evaluated at the disease-free equilibrium have negative real parts, which means that the disease-free equilibrium is locally asymptotically stable whenever the basic reproduction number is less than one ($\mathcal{R}_0 < 1$). Thus, we claim the following result.

Lemma 3.1. *The disease-free equilibrium x_0 is locally asymptotically stable if $\mathcal{R}_0 < 1$, and unstable otherwise.*

Item (ii) indicates the possibility of the appearance of the backward bifurcation phenomenon in the model (2.1) since the disease-free equilibrium can co-exist with two endemic equilibrium points whenever the basic reproduction number is less than one [25]. For further investigations on the subject, we will check the case (ii) of Theorem 3.3 by solving together equations $\mathcal{R}_0 < 1$ and $\mathcal{R}_c < 1$ in terms of A. We obtain that the case (ii) of Theorem 3.3 holds whenever,

$$\underbrace{\left(\frac{k_1 b\left[\epsilon\pi + \beta(1-\delta)(1-\gamma)\mu_3\right] + k_2\mu_3\left[\alpha(bk_1 + a)\right]}{\epsilon\pi + \beta(1-\delta)(1-\gamma)\mu_3}\right)}_{A_{\min}} < A_{\text{bif}} < \overbrace{\left(\frac{\mu_3 k_2(bk_1 + a)}{b(\epsilon\pi + \beta(1-\delta)(1-\gamma)\mu_3)}\right)}^{A_{\max}}. \tag{3.8}$$

We then claim the following result, which is a direct consequence of the item (ii) of Theorem 3.3.

Corollary 3.1. *If the condition* (3.8) *holds, then model* (2.1) *undergoes a backward bifurcation.*

3.5. Global stability analysis of steady states

3.5.1. Global stability of the disease-free equilibrium in a particular case

Letting us consider that the saturation parameter b that measures the effect of the delay in treatment for the infected individuals is equal to zero, that is $b = 0$. Thus, considering only the infected compartments of system (2.1), we obtain

$$\begin{pmatrix} \frac{dI}{dt}(t) \\ \frac{dB}{dt}(t) \end{pmatrix} = (F - V)\begin{pmatrix} I(t) \\ B(t) \end{pmatrix} - \mathcal{M}(S, I, B), \tag{3.9}$$

where $F = \begin{pmatrix} \frac{\delta_1\gamma_1 A\beta}{k_2} & \frac{A\pi}{k_2} \\ 0 & 0 \end{pmatrix}$, $V = \begin{pmatrix} k_1 & 0 \\ -\varepsilon & \mu_3 \end{pmatrix}$, and $\mathcal{M}(S, I, B) = \begin{pmatrix} (\beta\gamma_1\delta_1 I + \pi B)(S_0 - S) + a \\ 0 \end{pmatrix}$. In Υ, $S_0 \geq S(t)$ for all $t > 0$. Then, it follows that $\mathcal{M}(S, I, B) \geq \mathbf{0}_{\mathbb{R}^2}$. This means that

$$\begin{pmatrix} \frac{dI}{dt}(t) \\ \frac{dB}{dt}(t) \end{pmatrix} \leq (F - V)\begin{pmatrix} I(t) \\ B(t) \end{pmatrix}.$$

Note that

$$V^{-1} = \begin{pmatrix} \frac{1}{k_1} & 0 \\ \frac{\varepsilon}{k_1\mu_3} & \frac{1}{\mu_3} \end{pmatrix} \geq \mathbf{0}_{\mathbb{R}^{2\times 2}}.$$

We also have $F \geq 0$. Thus, from [26, Theorem 2.1], there exists a Lyapunov function for system (2.1) expressed as $L(S, I, B) = u'V^{-1}(I, B)'$ where u' is the left eigenvector of the nonnegative matrix $V^{-1}Z$ corresponding to the eigenvalue $\mathcal{R}_0$. This implies that,

$$\frac{dL}{dt} = (\mathcal{R}_0 - 1)\, u'(I, B) - u'V^{-1}\mathcal{M}(I, B) \leq 0.$$

Since $\mathcal{M}(S, I, B) \geq (0, 0)'$, it follows that $\frac{dL}{dt} < 0$ whenever $\mathcal{R}_0 < 1$, with $\frac{dL}{dt} = 0$ if and only if $(I, B) = (0, 0)$. It follows that the largest invariant set contained in $\left\{(S, I, B) \in \mathbb{R}^3_+ : \frac{dL}{dt} = 0\right\}$ is $\{x_0\}$. Thus, from LaSalle Invariance Principle [27], every solution of (2.1) with initials conditions in Υ converge to x_0 when $t \longrightarrow +\infty$. That is $(I, B) \longrightarrow (0, 0)$, and $S \longrightarrow S_0$ when $t \longrightarrow +\infty$, which is equivalent to $(S, I, B) \longrightarrow (S_0, 0, 0)$ when $t \longrightarrow +\infty$. Thus, the disease-free equilibrium x_0 is globally asymptotically stable in Υ whenever $\mathcal{R}_0 < 1$. We thus claim what follows:

Theorem 3.4. *If the saturation parameter b that measures the effect of the delay in treatment for the infected individuals is equal to zero, that is $b = 0$, then the disease-free equilibrium x_0 is globally asymptotically stable in Υ whenever $\mathcal{R}_0 < 1$.*

3.5.2. Global stability of the endemic equilibrium point

Our goal here is to prove the global stability of the unique endemic equilibrium x^* when $R_0 > 1$, using the geometric approach [28]. To this aim, we'll start with a quick overview of the procedure's general mathematical foundation, as devised by Li and Muldowney [28, 29].

Suppose the map $f(w)$ is a C^1 function for w in an open subset $P \subset R^n$, and consider the following autonomous dynamical system:

$$w^{'} = f(w). \tag{3.10}$$

Let $w(t, w_0)$ be the solution to Eq (3.10) satisfying $(0, w_0) = w_0$. Now we're going to make some fundamental assumptions:

(a) There is a tiny absorption set $K \subset P$ available;
(b) In a simply connected P, the ordinary differential system (3.10) has a single steady state w^*.

According to the preceding assumptions (a)–(b), if a point w is locally stable and all trajectories in P converge to the same point, w, it is said to be globally stable in P. That is, there are no non constant periodic solutions in system (3.10). It's worth noting that the Bendixson criteria play a vital part in determining global stability. A Bendixson criterion for $n \geq 2$ is a condition provided by field f that prevents non constance periodic solutions of equations from existing (3.10). The typical outcomes (see [30]) provide suitable global conditions for $n = 2$ (i.e., the planar case). In the work of Li and Muldowney [28], a surprising approach for showing global stability for $n \geq 3$ may be traced. They demonstrated in their study that if the criteria (a)–(b) are met and ordinary differential system (3.10) fulfills a Bendixson condition that holds up under pressure C^1 local f perturbations at all non-equilibrium non-wandering places for system (3.10), then w^* is globally stable in P and stable in addition. We present the Bendixson criteria, which are based on the Lozinski measure proposed in [29] and are robust to C^1 local *upsilon*-perturbations. Consider the ordinary differential system (3.10) given the following criteria (a) to (b). Let $D(w)$ be a $C_2^n \times C_2^n$ matrix-valued function which is C^1 for $w \in P$, and consider

$$A = D_f D^{-1} + DJ^{[2]}D^{-1}, \tag{3.11}$$

where D_f is P's directional derivative in the vector field's direction. f in system (3.10), and $J^{[2]}$ is so-called that the second additive compound matrix of J. Consider the following amount, q_2, which is written as

$$q_2 = \lim_{t\to\infty} \sup_{w_0\in\Omega} \frac{1}{t} \int_0^t \rho(A(s, w_0))ds, \tag{3.12}$$

where $\rho(A)$ is the Lozinski measure of A with respect to vector norm $|.|$ in R^N, $N = C(n, 2)$. (For more information, check [31]. They established in their study [29] that if the hypothesis (a) and (b) are satisfied, then $q_2 < 0$, suggesting that no orbits (periodic orbits, homoclinic orbits, and heteroclinic cycles) generate a simple closed rectifiable curve in D that is system invariant (3.10). Furthermore, number $q_2 < 0$ signifies the local stability of equilibrium point w under the specified hypothesis (a)–(b), as stated in [29]. Theorem 3.3 follows as a result.

Assuming that the hypothesis (a) to (b) hold and let $w = (S, I, B)$. Let $f(w)$ be the vector field of system (2.1). The second additive compound matrix $J^{[2]}$ of The Jacobian matrix $\mathcal{J} = \left[\mathcal{J}_{ij}\right]_{(3\times3)} = \partial f/\partial w$ associated with a general solution $w(t)$ of our system (2.1) is given by

$$\mathcal{J}^{[2]} = \begin{pmatrix} J_{11} + J_{22}, & \pi S, & \pi S \\ \varepsilon, & J_{11} + J_{33}, & -\dfrac{\alpha A}{(1+\alpha I)^2} - \beta\gamma_1\delta_1 S + \dfrac{ab}{(b+I^*)^2} \\ 0, & \beta\gamma_1\delta_1 I + \pi B, & J_{22} + J_{33} \end{pmatrix}. \tag{3.13}$$

Choosing the function

$$P = P(S, I, B) = diag(1, I/B, I/B),$$

then

$$P_f P^{-1} = diag\left(0, \frac{I^{'}}{I} - \frac{B^{'}}{B}, \frac{I^{'}}{I} - \frac{B^{'}}{B}\right).$$

So, by forward computation of (3.11) we get

$$A = [A_{ij}] = \begin{pmatrix} J_{11} + J_{22}, & \pi S, & \pi S \\ \varepsilon, & J_{11} + J_{33} + \frac{I^{'}}{I} - \frac{B^{'}}{B}, & -\frac{\alpha A}{(1+\alpha I)^2} - \beta\gamma_1\delta_1 S + \frac{ab}{(b+I^*)^2} \\ 0, & \beta\gamma_1\delta_1 I + \pi B, & J_{22} + J_{33} + \frac{I^{'}}{I} - \frac{B^{'}}{B} \end{pmatrix}. \tag{3.14}$$

The matrix A can be rewritten as a block matrix: $A_{11} = J_{11} + J_{22},\ A_{12} = (\pi S, \pi S),\ A_{21} = (\varepsilon, 0)^T$ and

$$A_{22} = \begin{pmatrix} J_{11} + J_{33} + \frac{I^{'}}{I} - \frac{B^{'}}{B}, & -\frac{\alpha A}{(1+\alpha I)^2} - \beta\gamma_1\delta_1 S + \frac{ab}{(b+I^*)^2} \\ \beta\gamma_1\delta_1 I + \pi B, & J_{22} + J_{33} + \frac{I^{'}}{I} - \frac{B^{'}}{B} \end{pmatrix}. \tag{3.15}$$

Letting (u_1, u_2, u_3) be a vector in $\mathbb{R}^3_+$; its norm $\|.\|$ is defined as

$$\|(u_1, u_2, u_3)\| = \max_{t\to\infty} \{|u_1|, |u_2| + |u_3|\}. \tag{3.16}$$

We use the Lozinskii measure $\mu(A)$ in relation to the norm (3.16) as

$$\mu(A) < \sup\{g_1, g_2\}, \tag{3.17}$$

where $g_1 = \hat{\mu}(A_{11}) + |A_{12}|,\ g_2 = \hat{\mu}(A_{22}) + |A_{21}|, |A_{12}|, |A_{22}|$ are matrix norms in terms of I_1 vector norms, and $\hat{\mu}$ is the Lozinskili measure in terms of this norm I_1.; then $\hat{\mu}(A_{11}) = -\beta\gamma_1\delta_1 I^* - \pi B^* - k_2 + \beta\gamma_1\delta_1 S^* - k_1 - \frac{ab}{(b+I^*)^2},\ |A_{12}| = \pi S,\ |A_{21}| = \varepsilon$. By adding both non-diagonal components of every column of A_{22} to the corresponding columns of the diagonal elements, one get $\hat{\mu}(A_{22})$,

$$A^{'}_{22} = \begin{pmatrix} -k_2 - \mu_3 + \frac{I^{'}}{I} - \frac{B^{'}}{B}, & -\frac{\alpha A}{(1+\alpha I)^2} - \beta\gamma_1\delta_1 S + \frac{ab}{(b+I^*)^2} \\ \beta\gamma_1\delta_1 I + \pi B, & -\frac{\alpha A}{(1+\alpha I)^2} - \mu_3 + \frac{I^{'}}{I} - \frac{B^{'}}{B} \end{pmatrix}. \tag{3.18}$$

Hence, to find $\hat{\mu}(A_{22})$, as the sum of the maximum of two diagonal cells of $A^{'}_{22}$:

$$\begin{aligned} \hat{\mu}(A_{22}) &= \max\left\{-k_2 - \mu_3 + \frac{I^{'}}{I} - \frac{B^{'}}{B}, -\frac{\alpha A}{(1+\alpha I)^2} - \mu_3 + \frac{I^{'}}{I} - \frac{B^{'}}{B}\right\} \\ &= -\frac{\alpha A}{(1+\alpha I)^2} - \mu_3 + \frac{I^{'}}{I} - \frac{B^{'}}{B}, \end{aligned}$$

provided that $\frac{\alpha A}{(1+\alpha I)^2} \leq k_2$. So, $g_1 = -\beta\gamma_1\delta_1 I^* - k_2 + \beta\gamma_1\delta_1 S^* - k_1 - \frac{ab}{(b+I^*)^2}$, $g_2 = \varepsilon - \frac{\alpha A}{(1+\alpha I)^2} - \mu_3 + \frac{I'}{I} - \frac{B'}{B}$.

To be mathematically and biologically reasonable, we will assume that

$$\mu(A) \leq \sup\{g_1, g_2\} \leq \varepsilon - \frac{\alpha A}{(1+\alpha I)^2} - \mu_3 + \frac{I'}{I} - \frac{B'}{B}.$$

Since, the $\sup_{t\to\infty} I(t) = \frac{A}{k_2}$, it is easy to verify that

$$\mu(A) \leq \frac{I'}{I} - \left(\frac{k_2^2\alpha A}{(k_2+\alpha A)^2} - \varepsilon\right). \tag{3.19}$$

So, from 0 to t, integrating both sides of (3.19) as

$$\frac{1}{t}\int_0^t \mu(A) \leq \frac{1}{t}\ln\frac{I(t)}{I(0)} - \left(\frac{k_2^2\alpha A}{(k_2+\alpha A)^2} - \varepsilon\right). \tag{3.20}$$

Then,

$$\limsup_{t\to\infty} \frac{1}{t}\int_0^t \mu(A) \leq -\left(\frac{k_2^2\alpha A}{(k_2+\alpha A)^2} - \varepsilon\right) < 0. \tag{3.21}$$

Hence, the global stability of the unique endemic equilibrium point x^* is investigated according to the geometric approach. The following theorem gives sufficient conditions for our aim.

Theorem 3.5. *The unique positive point x^* is asymptotically stable globally whenever $\mathcal{R}_0 > 1$ provided that*

$$\varepsilon < \frac{k_2^2\alpha A}{(k_2+\alpha A)^2} < k_2. \tag{3.22}$$

Remark 3.1. It is important to note that we can also use the techniques developed in [32] to also obtain the proof of the global stability of the unique endemic equilibrium point whenever the basic reproduction number is greater than one.

4. Numerical results and simulations

For numerical simulations, we consider the parameter values consigned in Table 2.

Table 2. Parameter values used in numerical simulation.

Parameter	Values	Parameter	Values
A	25	μ_1, μ_2	1/60
β	0.21	μ_3	0.03
γ	0.75	a	1
δ	0.75	b	1
α	0.2	μ_I	10^{-4}
π	0.5	ϵ	0.1

With theses values, we obtain $\mathcal{R}_0 = 27.23228 > 1$, $\mathcal{R}_c = 0.008620 < 1$ and the polynomial (3.3) becomes

$$I\left(-1.68987041 \times 10^{-4} I^3 - 0.00116649 I^2 + 1.24898335 I + 1.21358086\right) = 0, \tag{4.1}$$

which validates the case (iv) of Theorem 3.3. Now, we take $A = 0.2$ and the other parameters have the same values consigned in Table 2. We thus obtain $\mathcal{R}_0 = 0.2178582326436636 < 1$, $\mathcal{R}_c = 1.077553784778204 > 1$ and the polynomial (3.3) becomes

$$I\left(-1.68987041 \times 10^{-4} I^3 - 0.00116649 I^2 - 7.81645208 \times 10^{-4} I - 0.03618413\right) = 0, \tag{4.2}$$

which validates the case (i) of Theorem 3.3.

Setting $A = 0.9180$ and leave the other parameters as in Table 2, we obtain $\mathcal{R}_0 = 1$, $\mathcal{R}_c = 0.2347 < 1$ and the polynomial (3.3) becomes

$$I^2\left(-1.689870416666666 \times 10^{-4} I^2 - 0.001166498916666666 I + 0.035402488125\right) = 0, \tag{4.3}$$

which validates as well as the case (iii) of Theorem 3.3. Now, we verify condition (3.8) (case (ii) of Theorem 3.3). Leaving all model parameter values as in Table 2, we have $A_{\min} = 0.2155$ and $A_{\max} = 0.9180$. Thus, simply choosing $A_{\text{bif}} = 0.9$, we obtain $\mathcal{R}_0 = 0.9803 < 1$, $\mathcal{R}_c = 0.23948 < 1$ and the polynomial (3.3) becomes

$$I\left(-1.6898 \times 10^{-4} I^3 - 0.0011 I^2 + 0.0344 I - 9.0850 \times 10^{-4}\right) = 0, \tag{4.4}$$

which means that the backward bifurcation phenomenon can occurs in model (2.1).

We then illustrates the above result graphically. On Figure 2, we see that for $\mathcal{R}_0 < 1$, trajectories of infected states tend to zero, i.e, to the disease free equilibrium. By cons, on Figure 5, it is clear that for $\mathcal{R}_0 > 1$, trajectories of infected states tend the endemic equilibrium.

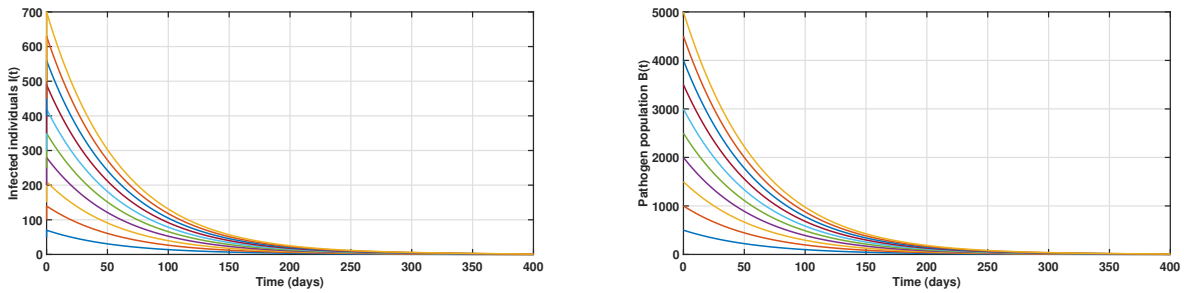

Figure 2. Time series of infected compartments for $\mathcal{R}_0 < 1$.

The backward bifurcation phenomenon is depicted in Figures 3 and 4. We see that Although the basic reproduction number is less than one, infected states tend to the endemic state.

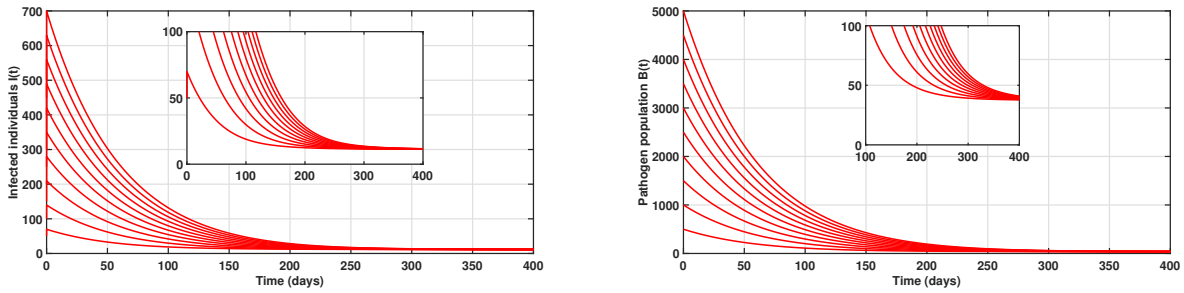

Figure 3. Time series of infected compartments for $\mathcal{R}_c < \mathcal{R}_0 < 1$.

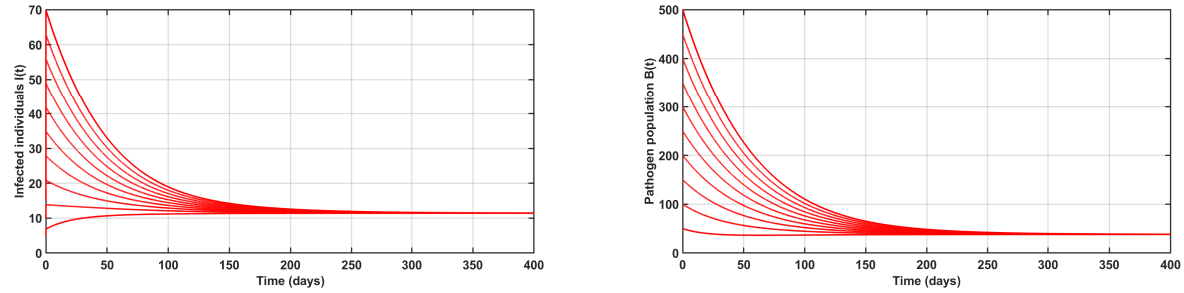

Figure 4. Time series of infected compartments for $\mathcal{R}_0 = 1$.

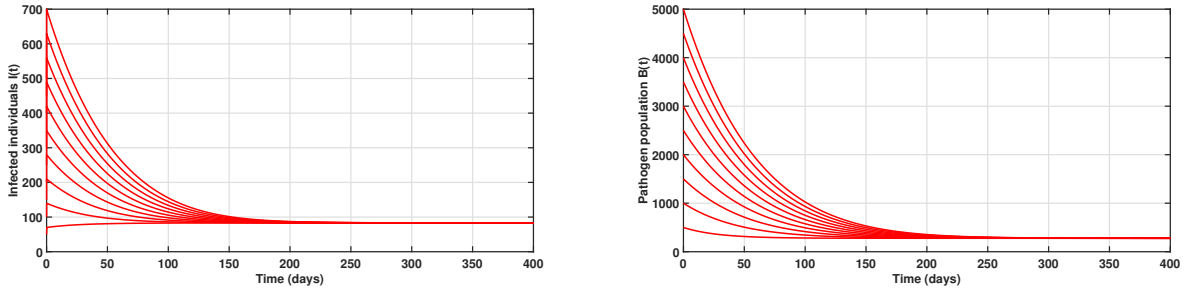

Figure 5. Time series of infected compartments for $\mathcal{R}_0 > 1$.

We pursue this part of the work by study numerically the impact of some model parameters like α, A, on the disease dynamics. For this aim, we vary the fear parameter α between 0 and 0.06 ($0 \leq \alpha \leq 0.06$). The result is depicted in Figures 6 and 7. It is clear that when the fear increases, the number of infected individuals decrease considerably Figure 6. This prove that media campaigns which show the negative effects of COVID-19 have a best effect to stop the spread ot the virus into human communities. Also, Figure 7 shows that control measures consisting to limit the population movements (quarantine and confinement) can also permit to decrease in the number of COVID-19 cases in the population.

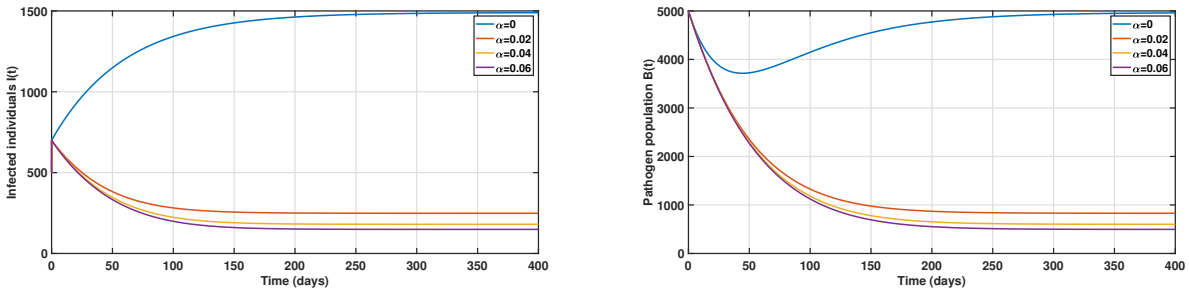

Figure 6. Time series of infected compartments with the variation of the fear parameter α.

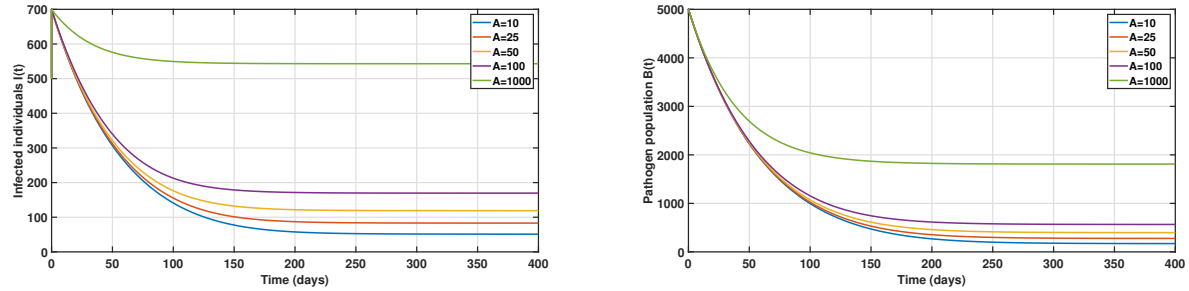

Figure 7. Time series of infected compartments with the variation of the recruitment parameter A.

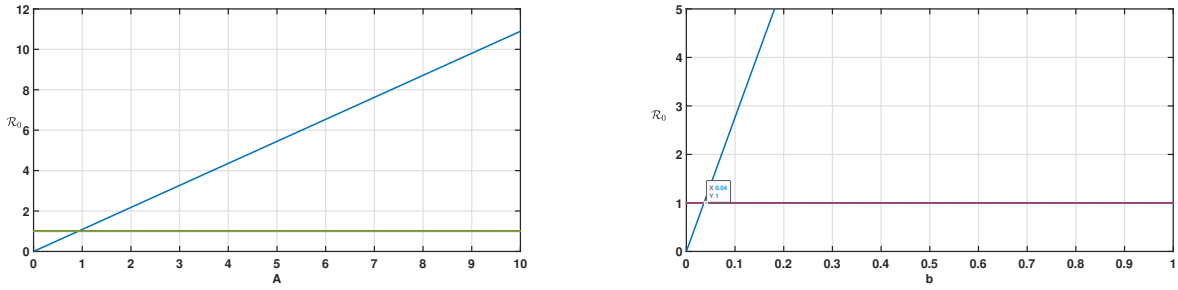

(a) (b)

Figure 8. The basic reproduction number function of (a) the recruitment rate A; (b) the saturation factor.

Figure 8 shows the basic reproduction number in terms of the recruitment rate (panel left) and the saturation Factor (right panel). We see that Ro IS an increasing function of these two model parameters. Indeed when $A > 0.96$, then $Ro > 1$ and Figure 9 shows the 3D representation as well as the contour plot of the basic reproduction number, function of the recruitment rate A and the saturation factor b. We note that these two parameter plays an important role in the disease dynamics. Indeed, increasing b while decreasing A permits to decrease in the value of the basic reproduction number, and thus, the number of new cases.

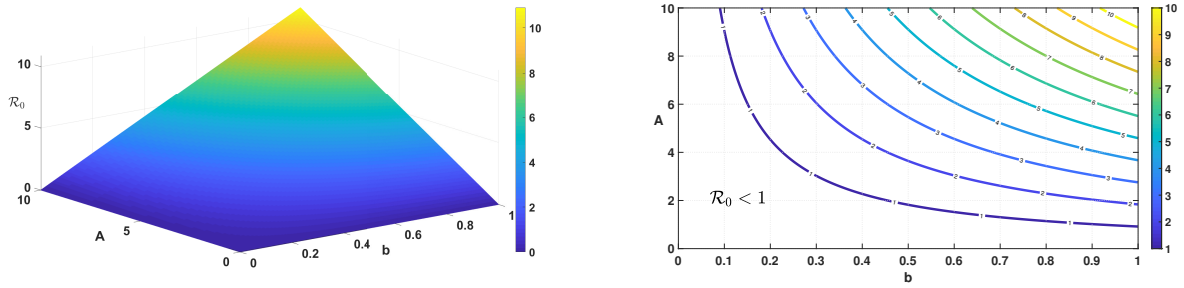

Figure 9. 3-D plot of the basic reproduction number, function of the recruitment rate A and the saturation factor b, and the corresponding contour plot.

5. Conclusions

In this study, we looked into a mathematical SIS-B model of COVID-19 with a fear impact and saturated treatment function. We investigated dynamical behavior, such as the stability of disease-free equilibrium and endemic equilibrium, using the comparison theorem and the second additive compound matrix theory. We often decrease the fundamental reproduction number below unity to eradicate the disease. This criterion, however, is insufficient in our model. In fact, we discovered a circumstance under which the model's backward bifurcation could occur. However, if we set the saturation parameter, which gauges the impact of delaying treatment for sick people, to zero, this phenomena vanishes. So, using the comparison theorem, we proved that the disease-free equilibrium is globally asymptotically stable whenever the basic reproduction is less than one. We may deduce from the previous study, the limited treatment capacity is a major cause of backward bifurcation. As a result, if we want to eradicate COVID-19 in a certain location, we must increase medical facilities in hospitals, such as increasing beds and providing enough treatment medicine. We also prove the global stability of the unique endemic equilibrium whenever $\mathcal{R}_0$ is greater than one, using the geometric approach. Further methods studied in [32] can also be used to prove the global stability of the endemic equilibrium whenever the basic reproduction number is greater than one.

To the best of our knowledge, the impact of fear on susceptible people from infected people has not been investigated. After conducting considerable research on this topic, it was discovered that the impact of fear on the disease dynamics has an important effort. For this aim, we vary the fear parameter α between 0 and 0.6 ($0 \leq \alpha \leq 0.06$). The result, depicted through numerical simulations (see Figure 6), shows that it is clear that when the fear increases, the number of infected individuals decreases considerably. This proves that media campaigns that show the negative effects of COVID-19 have the best effect to stop the spread of the virus into human communities.

Acknowledgments

The authors Aziz Khan and Thabet Abdeljawad would like to thank Prince Sultan University for the support through the research lab TAS.

Conflict of interest

The authors declare no conflict of interest.

References

1. K. Bjørkdahl, B. Carlsen, Fear of the fear of the flu: Assumptions about media effects in the 2009 pandemic, *Sci. Commun.*, **39** (2017), 291–410. https://doi.org/10.1177/1075547017709792
2. I. Ghosh, P. K. Tiwari, S. Samanta, I. M. Elmojtaba, N. Al-Salti, J. Chattopadhyay, A simple SI-type model for HIV/AIDS with media and self-imposed psychological fear, *Math. Biosci.*, **306** (2018), 160–169. https://doi.org/10.1016/j.mbs.2018.09.014
3. The World Bank, Fertility rate, total (births per woman)-Hong Kong SAR, china, 2018. Available from: https://data.worldbank.org
4. J. Hiscott, M. Alexandridi, M. Muscolini, E. Tassone, E. Palermo, M. Soultsioti, et al., The global impact of the coronavirus pandemic, *Cytokine Growth Factor. Rev.*, **53** (2020), 1–9. https://doi.org/10.1016/j.cytogfr.2020.05.010
5. R. Glaser, T. F. Robles, J. Sheridan, W. B. Malarkey, J. K. KiecoltGlaser, Mild depressive symptoms are associated with amplified and prolonged inflammatory responses after influenza virus vaccination in older adults, *Arch. Gen. Psychiatry*, **60** (2003), 1009–1014. https://doi.org/10.1001/archpsyc.60.10.1009
6. K. Roosa, Y. Lee, R. Y. Luo, A. Kirpich, R. Rothenberg, J. M. Hyman, et al., Short-term forecasts of the COVID-19 epidemic in Guangdong and Zhejiang, China: February 13–23, 2020, *J. Clin. Med.*, **9** (2020), 596. https://doi.org/10.3390/jcm9020596
7. N. Nuraini, K. Khairudin, M. Apri, Modeling simulation of COVID-19 in Indonesia based on early endemic data, *Commun. Biomathematical Sci.*, **3** (2020). http://doi.org/10.5614/cbms.2020.3.1.1
8. R. C. Das, Forecasting incidences of COVID-19 using Box-Jenkins method for the period July 12-Septembert 11, 2020: A study on highly affected countries, *Chaos Solitons Fractals*, **140** (2020), 110248. https://doi.org/10.1016/j.chaos.2020.110248
9. A. Ajbar, R. T. Alqahtani, Bifurcation analysis of a SEIR epidemic system with governmental action and individual reaction, *Adv. Difference Equ.*, **2020** (2020), 541. https://doi.org/10.1186/s13662-020-02997-z
10. M. Sher, K. Shah, Z. A. Khan, H. Khan, A. Khan, Computational and theoretical modeling of the transmission dynamics of novel COVID-19 under Mittag-Leffler Power law, *Alex. Eng. J.*, **59** (2020), 3133–3147. https://doi.org/10.1016/j.aej.2020.07.014
11. M. A. Dokuyucu, E. Celik, Analyzing a novel coronavirus model (COVID-19) in the sense of Caputo-Fabrizio fractional operator, *Appl. Comput. Math. Ean Int. J.*, **20** (2021), 49–69.
12. M. A. Khan, A. Atangana, E. Alzahrani, Fatmawati, The dynamics of COVID-19 with quarantined and isolation, *Adv. Difference Equ.*, **2020** (2020), 425. https://doi.org/10.1186/s13662-020-02882-9
13. S. K. Panda, Applying fixed point methods and fractional operators in the modelling of novel coronavirus 2019-nCoV/SARS-CoV-2, *Results Phys.*, **19** (2020), 103433. https://doi.org/10.1016/j.rinp.2020.103433

14. H. Mohammadi, S. Kumar, S. Rezapour, S. Etemad, A theoretical study of the Caputo–Fabrizio fractional modeling for hearing loss due to Mumps virus with optimal control, *Chaos Solitons Fractals*, **144** (2021), 110668. https://doi.org/10.1016/j.chaos.2021.110668

15. C. Maji, Impact of media-induced fear on the control of COVID-19 outbreak: A mathematical study, *Int. J. Differ. Equ.*, **2021** (2021), 2129490. https://doi.org/10.1155/2021/2129490

16. S. C. Mpeshe, N. Nyerere, Modeling the dynamics of coronavirus disease pandemic coupled with fear epidemics, *Comput. Math. Methods Med.*, **2021** (2021), 6647425. https://doi.org/10.1155/2021/6647425

17. L. L. Zhou, S. Ampon-Wireko, X. L. Xu, P. E. Quansah, E. Larnyo, Media attention and vaccine hesitancy: Examining the mediating effects of fear of covid-19 and the moderating role of trust in leadership, *Plos one*, **17** (2022), e0263610. https://doi.org/10.1371/journal.pone.0263610

18. S. V. Scarpino, G. Petri, On the predictability of infectious disease outbreaks, *Nat. Commun.*, **10** (2019), 898. https://doi.org/10.1038/s41467-019-08616-0

19. A. I. K. Butt, W. Ahmad, M. Rafiq, D. Baleanu, Numerical analysis of Atangana-Baleanu fractional model to understand the propagation of a novel corona virus pandemic, *Alex. Eng. J.*, **61** (2022), 7007–7027. https://doi.org/10.1016/j.aej.2021.12.042

20. X. Zhang, X. N. Liu, Backward bifurcation of an epidemic model with saturated treatment function, *J. Math. Anal. Appl.*, **348** (2008), 433–443. https://doi.org/10.1016/j.jmaa.2008.07.042

21. W. Walter, *Ordinary Differential Equations*, Springer, 1998.

22. F. Sulayman, F. A. Abdullah, M. H. Mohd, An sveire model of tuberculosis to assess the effect of an imperfect vaccine and other exogenous factors, *Mathematics*, **9** (2021), 327. https://doi.org/10.3390/math9040327

23. X. Y. Zhou, X. Y. Shi, J. Cui, Stability and backward bifurcation on a cholera epidemic model with saturated recovery rate, *Math. Methods Appl. Sci.*, **40** (2017), 1288–1306. https://doi.org/10.1002/mma.4053

24. P. van den Driessche, J. Watmough, Reproduction numbers and sub-threshold endemic equilibria for compartmental models of disease transmission, *Math. Biosci.*, **180** (2002), 29–48. https://doi.org/10.1016/s0025-5564(02)00108-6

25. H. Abboubakar, J. C. Kamgang, L. N. Nkamba, D. Tieudjo, Bifurcation thresholds and optimal control in transmission dynamics of arboviral diseases, *J. Math. Biol.*, **76** (2018), 379–427.

26. Z. S. Shuai, P. van den Driessche, Global stability of infectious disease models using Lyapunov functions, *SIAM J. Appl. Math.*, **73** (2013), 1513–1532. https://doi.org/10.1137/120876642

27. J. P. La Salle, The stability of dynamical systems, In: *CBMS-NSF regional conference series in applied mathematics*, 1976. https://doi.org/10.1137/1.9781611970432

28. M. Y. Li, J. S. Muldowney, A geometric approach to global-stability problems, *SIAM J. Math. Anal.*, **27** (1996), 1070–1083. https://doi.org/10.1137/S0036141094266449

29. M. Y. Li, J. S. Muldowney, Global stability for the SEIR model in epidemiology, *Math. Biosci.*, **125** (1995), 155–164. https://doi.org/10.1016/0025-5564(95)92756-5

30. J. Guckenheimer, P. Holmes, *Nonlinear Oscillations, Dynamical Systems, and Bifurcations of Vector Fields*, Springer, 2002.

31. W. A. Coppel, *Stability and Asymptotic Behavior of Differential Equations*, D. C. Heath, 1965.

32. Y. K. Xie, Z. Wang, A ratio-dependent impulsive control of an siqs epidemic model with non-linear incidence, *Appl. Math. Comput.*, **423** (2022), 127018. https://doi.org/10.1016/j.amc.2022.127018

AIMS Press